Biofilm process in porous media - practical applications

Authors: Alfred B. Cunningham, B. Warwood, Paul J. Sturman, K. Horrigan, Garth A. James, J. William Costerton, Dwight R. Hiebert

This is a postprint of a book chapter that originally appeared in The Microbiology of the Terrestrial Deep Subsurface in 1997.

Cunningham, A., B. Warwood, P. Sturman, K. Horrigan, G. James, J.W. Costerton, and R. Hiebert, “Biofilm Process in Porous Media - Practical Applications,” In: P.S. Amy, D.L. Haldeman (eds), The Microbiology of the Terrestrial Deep Subsurface, Lewis Publishers, 1997, Chapter 17, pp. 325-344.

The Microbiology of the Terrestrial Deep Subsurface

Edited by

Penny S. Amy
Dana L. Haldeman

LEWIS PUBLISHERS
Boca Raton New York

17

Biofilm Processes in Porous Media — Practical Applications

Al Cunningham, Bryan Warwood, Paul Sturman, Kevin Horrigan, Garth James, J. William Costerton, and Randy Hiebert

CONTENTS

KEY WORDS: *biobarrier, plugging, porous media, ultramicrobacteria, ground water, bioremediation, biofilm, containment, contaminants.*

17.1 Introduction

There are many microbial functions that are of interest to scientists and engineers who seek to manipulate processes in the subsurface environment. In bioremediation, we consider the capabilities of different groups of bacteria somewhat avidly because we know that these organisms can live in pore spaces in this environment and

0-8493-8362-5/97/$0.00+$.50

biodegrade organic pollutants and reduce metallic pollutants to an insoluble immobile form. In oil recovery, we are equally attracted to the well-established bacterial properties of plugging by slime (exopolysaccharide) production and of wax mobilization by surfactant production. There are literally dozens of potential uses for microorganisms in the subsurface and most of these involve bacteria because their small size (1 to 4 μm) makes them potentially more mobile in a porous medium than larger eukaryotic microorganisms.

The first attempts to use bacteria in the subsurface date back to the 1940s, in central Europe, when vegetative cells of a variety of potentially useful organisms were simply pumped down water injection wells with the intent of plugging the high-permeability "thief" zones that cause water breakthrough to the producing wells, and signal the end of effective secondary oil recovery. Success was claimed in some field experiments, but these well treatments were generally ineffective and the idea was largely abandoned. In 1984, the biofilm group at the University of Calgary undertook a controlled study of the transport of bacteria through porous media in cooperation with a geologist — Dr. Norman Wardlaw (Shaw et al., 1985). Pure monospecies and mixed natural populations of vegetative bacteria were passed into a porous medium composed of scintered glass beads whose pore throats averaged 27 μm. Direct examination by scanning electron microscopy (SEM) clearly showed that these vegetative cells adhered so avidly to the first available surfaces offered by the porous medium that they quickly plugged the inlet surface to produce a slimly "skin plug" only a few hundreds of microns deep. Direct examination was pivotal in this case because we could actually see the plugging phenomenon, which is very similar to biofilm formation in linear systems, and this process was not apparent to researchers extrapolating from culture data. Workers who had relied on culture methods, and had used bacteria that had been modified by repeated laboratory culture, found that some of these bacteria would pass through various porous media and be found and cultured at the effluent end of the matrix. When we used "wild-type" bacteria that had not lost their adherent properties during repeated lab culture, and when we used microscopy to examine the cells *in situ*, we proved that vegetative bacteria adhere avidly to available surfaces at the inlet of the matrix. This avid adhesion produces a *de facto* biofilm on the inlet surface which is heavily colonized, and even plugged, by metabolically active vegetative bacteria. This active population also may release a number of small starved bacteria that traverse the porous medium and emerge at the effluent end of the matrix. These small starved bacterial cells are well dispersed and they produce relatively large "counts" by traditional plating methods when the effluent fluids are cultured.

When metabolically active mixed populations of bacteria from the subsurface, in our case from "produced" water from a oil recovery operation, were introduced into a porous medium they adhered avidly to the first available surfaces and formed a very shallow "skin plug". Bacteria that had been cultured repeatedly were much more mobile in porous media because they had lost the tendency of wild-type bacteria to adhere to surfaces. It is clear that vegetative bacteria vary enormously in their adhesion capabilities and we must expect to find a spectrum of vegetative cells that span between the stickiness of wild-type biofilm bacteria, and the relative mobility of wild-type motile bacteria, to the higher mobility of cells that have lost their adhesive tendencies upon culture or have been genetically manipulated to delete enzymes involved in exopolysaccharide production. Mixed wild-type populations may be expected to contain cells in all of these states and slime formation by wild-type biofilm bacteria tends to trap cells of all types in the slimy "skin plug". We must also remember that wells that have received injection water containing live wild-type bacteria may already be extensively plugged by an existing skin plug (McKinley et al.,

1988) that will trap subsequently introduced organisms. We conclude that careful manipulation is necessary to deliver vegetative bacteria into the subsurface and that their penetration is inherently limited by their size (about 1.0 μm) and by at least some tendency to adhere to available surfaces.

Having concluded that "wild-type" metabolically active bacterial cells penetrate only very poorly through porous media, even though they are much smaller than the pore throats in those media, we turned to the study of the transport of ultramicrobacteria (UMB) through these same media. UMB were first described in the deep-sea environment by Morita and colleagues (Novitsky and Morita, 1976). They are simply bacterial cells that have undergone radical size reduction and adopted metabolic dormancy in response to starvation (see Chapter 11). In the very oligotrophic deep-sea environment, a wide variety of bacterial species respond to low levels of carbon and energy sources by a sigma factor-directed phenotypic change analogous to a bacterial stress response, in which they reduce their size (0.3 to 0.5 μm) and slow their metabolic processes until they approach complete dormancy (Kjelleberg, 1993). UMB are stable for many years, in the absence of nutrients, but they are capable of rapid resuscitation when suitable nutrients are supplied. These very small, dormant, starved bacterial cells have now been discovered in the deep subsurface (>8,000 ft) in formations where their presence clearly indicates that they are capable of free movement in porous media >150 milliDarcies (mD) in permeability. Because of their small size, their modified adhesion properties, and their capacity to form metabolically active vegetative cells through resuscitation, UMB appeared to constitute an ideal means of transporting bacteria with useful properties deep into the subsurface. A large number of aquatic and subsurface bacteria have been observed to form UMB, and a majority show this response to starvation (Kjelleberg, 1993). A minority of these bacteria form UMB that retain large cell envelopes with shrunken protoplasts, or form irregular-shaped UMB, and these UMB have no inherent advantages over most vegetative cells in terms of their penetration of porous media.

In the sections that follow we will describe experiments in which UMB can be seen to penetrate porous media (>110 mD in permeability) and respond to a suitable nutrient "chaser" by returning to the vegetative state, reproducing, and then producing exopolysaccharide to an extent that the pore spaces of the porous medium are completely occluded by bacterial biomass (McLeod et al., 1988). UMB derived from a variety of bacterial species have been shown to penetrate Berea sandstone cores and sand packs of various permeabilities, ranging from 1.4 Darcies (D) to >18 D. These UMB appear at the effluent end of the test system in small numbers at first, and then in numbers approaching those being injected at the inlet. Mass balance calculations and direct observations of fractured cores and sand samples have shown that some of the UMB that are introduced into porous media are retained in the pores, probably by simple trapping and by adsorption to the matrix material. Experiments conducted by the Alberta Research Council, using medium scale (45 cm diameter) oilfield simulators composed of sandpacks (1.4 D), indicated by extrapolation that UMB can penetrate at least 200 m through these consolidated sands (Cusack et al., 1992). The ability of UMB to readily penetrate porous media >110 mD, and the tendency of these small, dormant, starved cells to be retained within pore spaces as they are transported, sets the stage for resuscitation by nutrient "chasers".

UMB are not motile, and therefore they follow the path of injected water in the subsurface environment. They penetrate wherever pore sizes are permissive and a significant number are retained in each pore structure by trapping and/or adsorption. When a solution containing a suitable nutrient mixture for UMB resuscitation is subsequently injected into the porous medium, these nutrients "catch up " with the 0.3 to 0.5 μm UMB and initiate the relatively rapid process of resuscitation. The UMB return

to their vegetative 1.0 to 1.4 μm form and begin to reproduce by binary fission. Immediately following their resuscitation, vegetative bacteria derived from these UMB begin to produce exopolysaccharides (EPS) and the simultaneous nutrient-driven processes of reproduction and EPS production rapidly fill the available pore space if the nutrients provided are sufficient in concentration and readily assimilated (Lappin-Scott et al., 1988). The processes of resuscitation and plugging can be controlled by the judicious choice of nutrients that are fast-acting or slow-acting, by virtue of the extent to which they are assimilable by the resuscitating organisms, and by the rate at which these "wake up" nutrients are pumped into the porous medium in question. Rapid resuscitation of UMB, and slow rates of nutrient injection, can cause plugging very close to the injection point and limit the depth of the biobarrier that is put in place. We have been able to use modeling and other modern engineering tools to design UMB injection and resuscitation protocols that enable us to place biobarriers with considerable accuracy. The barriers to groundwater flow are attractive for environmental purposes because they form preferentially in zones of high permeability, and because they form in any part of the porous medium matrix that exceeds 110 mD in permeability. This latter characteristic is valuable because biobarriers formed by this method would actually be "anchored" in strata such as highly permeable sandstone. Biobarriers would avoid the problems of physical barriers, such as sheet piling and grout, which are readily bypassed by groundwater that flows between them and the underlying bedrock.

Because biobarriers can be constructed from the virtually limitless armamentarium of bacterial species with different physiological capabilities, an almost infinite number of different types of barriers can be constructed. We will show that bacterial strains that reproduce readily and form large amounts of EPS can be used to construct "tight" biobarriers that plug 99.9% of groundwater flow and require subsequent nutrient addition less than every 110 years. On the other hand, biobarriers constructed using strains that produce very little EPS would plug the porous media of the subsurface to a much lesser extent and bacterial cells within these "loose" biobarriers would be capable of pollutant degradation and/or metal reduction as groundwater passed through them. Our present understanding of the microbiology of the subsurface environment has enabled us to devise a UMB-based technology to deliver bacteria of interest into specific regions of this environment for a wide variety of purposes ranging from virtually complete plugging to bioremediation and metal reduction. Perhaps the most reassuring aspect of this new technology is that it uses natural strains of subsurface bacteria in UMB and vegetative forms.

17.2 Biofilm Accumulation

In porous media, as in other aqueous environments, microbial cells may exist in suspension or may adsorb firmly to solid surfaces comprising the porous medium matrix. If favorable environmental conditions persist, adsorbed cells will grow and reproduce at the surface, increasing the amount of attached biomass. If rates of cell adsorption and growth exceed the rate of desorption, a net accumulation of biomass will result on the surface. As the accumulation process continues, additional cells may attach (and detach) directly to (or from) the existing biomass surface. Attachment and detachment are probably the least understood processes affecting the accumulation of biofilm. In this chapter we are concerned with the condition where the substrate

supply to the biofilm is sufficient to permit the formation of thick, continuous biofilms, as opposed to patchy, isolated cell colonies. The relationship between the substrate loading rate and biofilm morphology is discussed in detail by Rittmann (1993). Under high substrate loading conditions, the average biofilm thickness on individual media particles will increase, resulting in a corresponding decrease in effective pore space. In systems where the flow rate through the porous medium remains constant, the average pore velocity will increase with the increasing biofilm thickness, while in systems where the piezometric gradient remains constant, pore velocity will decrease. Increased thickness may result in depletion of nutrients within the biofilm structure. It is probable that the net rate of biofilm detachment increases with increasing biofilm thickness, but additional research is needed to fully confirm that assumption. However, it is clear that as the temporal progression of biofilm thickness reaches a quasi steady-state condition, the average specific growth rate for the biofilm must be balanced by the net detachment rate. Particles of organic and inorganic material flowing in suspension may be removed by the attached biomass through filtration processes including diffusion, interception, and sedimentation (Cunningham et al., 1990). The entire deposit of cells and polymers, together with captured organic and inorganic particles, is termed the "biofilm". The amount of biofilm accumulation occurring in a porous medium flow system is therefore the net result of the biomass added through adsorption, growth, attachment, and filtration, less the amount removed by desorption and detachment (Figure 17.1).

Individual biofilm processes are considerably more difficult to examine in porous media than in other common reactor geometries such as flasks, tanks, reservoirs, and pipelines. Biofilm growth, for example, is complicated by the nature of fluid and nutrient transport which, in porous media, occurs along tortuous flow paths of variable geometry. Similarly, the wide distribution of pore velocities introduces considerable variation in the processes of adsorption, desorption, attachment, and detachment.

17.3 Microscale Observations

The accumulation and activity of biofilms varies from point to point along individual pore channels, and thus are considered to be microscale phenomena. Observations of biofilm processes have been reported by several investigators. Cunningham et al. (1991) conducted microscopic observations of porous media biofilm reactors under high substrate loading conditions (25 mg l^{-1}). Media tested consisted of 1 mm glass spheres, 0.70 mm sand, 0.54 mm sand, and 0.12 mm glass and sand. *Pseudomonas aeruginosa* was used as the inoculum and 25 mg l^{-1} glucose substrate was continuously supplied to the reactor. Reactors were operated under constant piezometric head conditions resulting in a flow rate decrease as a biofilm developed. Biofilm accumulation was measured by determining the average thickness on the exposed edges of individual media particles (Figure 17.2). The progression of biofilm thickness followed a sigmoidal curve, reaching a maximum thickness after about 5 days, and maximum thickness was proportional to medium diameter (Cunningham et al., 1991).

Wanner et al. (1995) investigated microscale biofilm accumulation in a packed-bed biofilm reactor inoculated with a pure culture of *P. aeruginosa* that was run under high substrate loading and constant flow rate conditions. The 3.1-cm-diameter cylindrical reactor was 5 cm in length and packed with 1 mm glass beads. Daily observations of

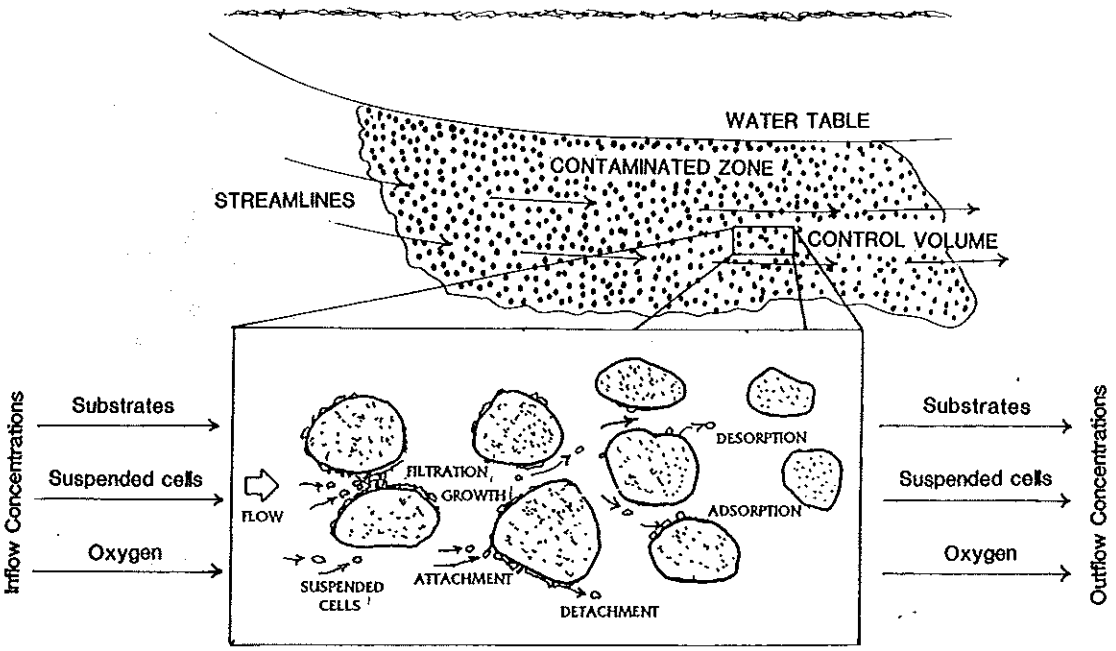

FIGURE 17.1
Schematic showing individual processes contributing to biofilm accumulation and detachment in porous media.

FIGURE 17.2
Pseudomonas aeruginosa biofilm growing on the exposed edges of 150 µm sand grains. The biofilm is the light-colored material attached to the dark-colored sand grains.

biofilm thickness, influent and effluent glucose substrate concentration, and effluent dissolved and total organic carbon were made during the 13-day experiment. Biofilm thickness appeared to reach a quasisteady-state condition after 10 days. AQUASIM, a published biofilm process simulation program (Reichert, 1994), was used to analyze the experimental data. Comparison of observed and simulated variables revealed three distinct phases of biofilm accumulation during the experiment: (1) an initial

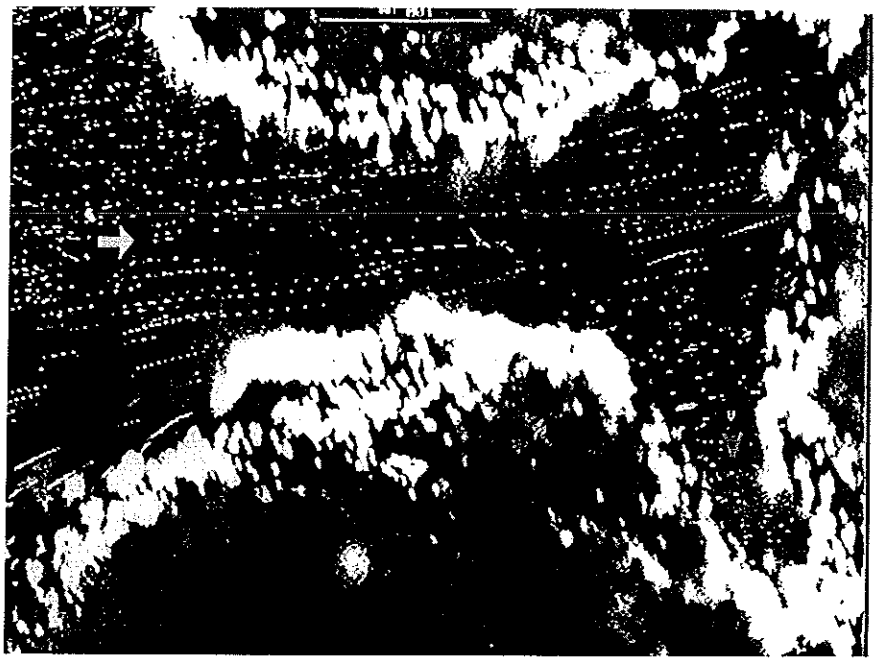

FIGURE 17.3
Streak lines through a porous medium-biofilm matrix. Local fluid velocity was measured by particle image velocimetry using 0.282 μm latex beads and scanning confocal laser microscopy. The arrow indicates the direction of flow. Beads that were transported rapidly were captured by time-lapse photography as strings of beads, while in areas of virtually no flow, where beads demonstrated little or no movement, they were captured as a single bead, or slightly elongated bead.

phase in which substrate removal is determined by cell mass and mass transfer resistance between biofilm and bulk fluid, (2) a growth phase in which cell mass, mass transfer resistance, and area of the biofilm-bulk fluid interface are important, and (3) a mature biofilm phase in which the area of the interface is the important parameter. In this last phase mass transfer resistance between the biofilm and the bulk fluid is insignificant and the biofilm thickness has little effect on the substrate removal rate. It was also found that, in a porous medium under high substrate loading, biofilm detachment is correlated with shear stress at the biofilm surface.

Development of the confocal scanning laser microscope has allowed more detailed examinations of live biofilms under flowing conditions. Stoodley et al. (1994) investigated liquid flow in a model biofilm system consisting of *P. aeruginosa*, *P. fluorescens*, and *Klebsiella pneumoniae*. Local fluid velocity was measured by particle image velocimetry (neutral density 0.282 μm latex spheres) and scanning confocal laser microscopy. Figure 17.3 shows the streaklines defined by the latex spheres flowing between two 250-μm-diameter glass beads in the porous medium flow cell reactor. A biofilm approximately 30 μm in thickness had accumulated on the exposed edges of the beads. Analysis of particle velocity data indicates that as biofilm accumulates in a porous medium it can have a significant effect on local flow velocities and shear stresses. Some channels may become completely blocked while some are only partially restricted.

17.4 Influence on Hydrodynamics

The foregoing experimental investigations indicate that as biofilm thickness increases, the diffusional path length within the biofilm increases, thereby decreasing

nutrient concentrations in the base film which will subsequently reduce growth rate. Accumulation of biofilm will continue until the specific growth rate is balanced by the detachment rate. These interactions give rise to the sigmoidal shape exhibited by the accumulation progressions, which indicate that a quasisteady-state thickness is eventually reached (Cunningham et al., 1991).

If sufficient biomass accumulates so as to reduce the effective pore space, a corresponding decrease in medium porosity and permeability as well as an increase in friction factor will ensue. Cunningham et al. (1991) observed that as thickness approached steady-state, medium porosity decreased between 50 and 96% while permeability decreased between 92 and 98%. The porous medium friction factor also increased substantially for all media tested. In all experimental results reported to date, observations of permeability in the biofilm-medium matrix indicate that a minimum permeability (3 to 7×10^{-8} cm^2) persisted after biofilm thickness had reached a maximum value. These observations suggest that, for the experimental conditions used herein, the biofilm accumulation process stabilizes so as to preserve a minimum permeability within the medium biofilm matrix. Such results indicate substantial interaction between mass transport, hydrodynamics, and biofilm accumulation at the fluid/biofilm interface in porous media.

17.5 Mesoscale Biobarrier Evaluation

Mesoscale evaluation of biobarrier formation and persistence was conducted in a series of column and small lysimeter reactors. Up-flow column reactors were used to study biobarrier development and long-term persistence in a one-dimensional flow configuration (nutrients and inocula provided in the hydraulic flow direction), and resistance to heavy metals and organic solvents. Lysimeter reactors were used to study biobarrier formation and persistence in two-dimensional flow systems (nutrients and inocula provided perpendicular to and independent from the hydraulic flow) and their resistance to heavy metals.

17.5.1 One-Dimensional Biobarrier Formation in Column Test Chambers

Test chambers consisted of 91.4-cm lengths of clear polyvinylchloride (PVC) pipe 15.2 cm in diameter. The chamber walls were coated with PVC adhesive and sand to limit bypass flow along the chamber walls. A column test chamber manufactured entirely from 316 stainless steel in the same dimensions as the PVC columns was used for organic solvent challenge work. The columns were packed with varying grades of foundry sand resulting in initial hydraulic conductivities of 0.26 to 2.97 cm/min. The chamber inlet and outlet were layered with large gravel, pea gravel, and course sand to prevent settling of sand into the inlet tubing and wash-out of sand from the outlet tubing. The chamber was fitted with 4 sample ports, spaced exponentially along the column at distances of 8.5, 18.2, 38.0, and 76.6 cm from the column inlet, to allow pressure measurements and withdrawal of fluid samples (Figure 17.4). Pressure was measured using piezometers located at each sample port. Flow of solutions through the chambers was provided by maintaining an 8-l constant-head tank approximately 2 m above the column inlet.

The hydraulic conductivity (K) of the column between each sample port was calculated using Darcy's law,

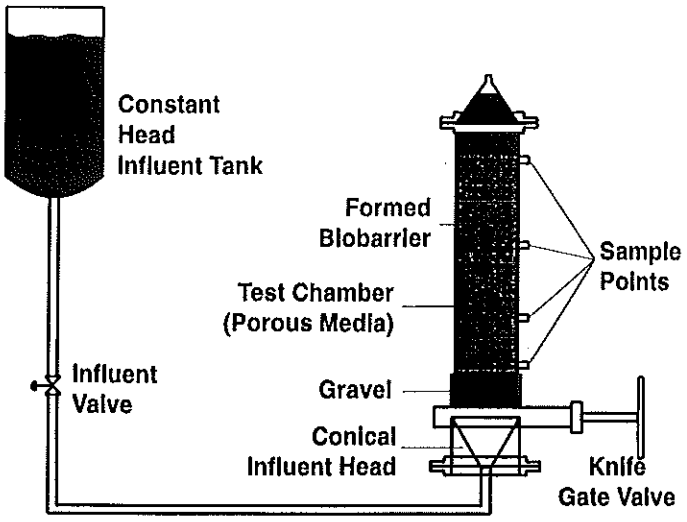

FIGURE 17.4
Sand-packed column for evaluation of biobarrier formation and performance. Nutrient and challenge solutions up-flow through the column from a constant-head reservoir.

$$K = Q/A\ (dh/dl) \tag{17.1}$$

where Q is the flow rate, A is the cross-sectional area of the column, and (dh/dl) is the piezometric gradient.

17.5.2 Inoculum Preparation and Column Inoculation

The inoculum for the nonsterile columns consisted of starved cells of a streptomycin-resistant environmental isolate of *Klebsiella oxytoca* suspended in a phosphate-buffered saline (PBS) solution (MacLeod et al., 1988). The bacterial culture was diluted in Sodium Citrate Medium (SCM; Lappin-Scott et al., 1988) to a volume equal to 2 column pore volumes and gravity fed to the column (final cell inoculum of 2.5×10^6 CFU/ml). The inoculated columns were then allowed to incubate under no-flow conditions for 2 days. Thereafter, the columns were perfused daily with SCM until the permeability became constant, after which the columns were continuously supplied with SCM.

Recoverable heterotrophic cells and streptomycin-resistant cells were enumerated in the column effluent during inoculation. Prior to the inoculation, the column effluent contained 1.4×10^5 CFU/ml recoverable heterotrophic cells and $<1 \times 10^3$ streptomycin-resistant cells. The columns were incoculated with a streptomycin-resistant *K. oxytoca* cell population at a concentration of approximately tenfold higher than the initial effluent cell population. Following inoculation, the effluent heterotrophic cell populations were not significantly higher than the initial effluent cell density; however, the number of streptomycin-resistant cells in the column effluent increased more than 100-fold. This result indicates that the streptomycin-resistant inoculum comprised a significant proportion of the culturable microbial community in the column, and in the column effluent. Following the inoculation and during nutrient resuscitation, the distribution of bacteria and nutrient concentrations were determined along the column length. These distributions indicated a homogeneous microbial recovery and effective biobarrier formation (Figures 17.5A and B).

Citrate utilization increased in proportion to the cell number increase, resulting in no detectable citrate throughout the column after 5 days. Phosphate concentrations

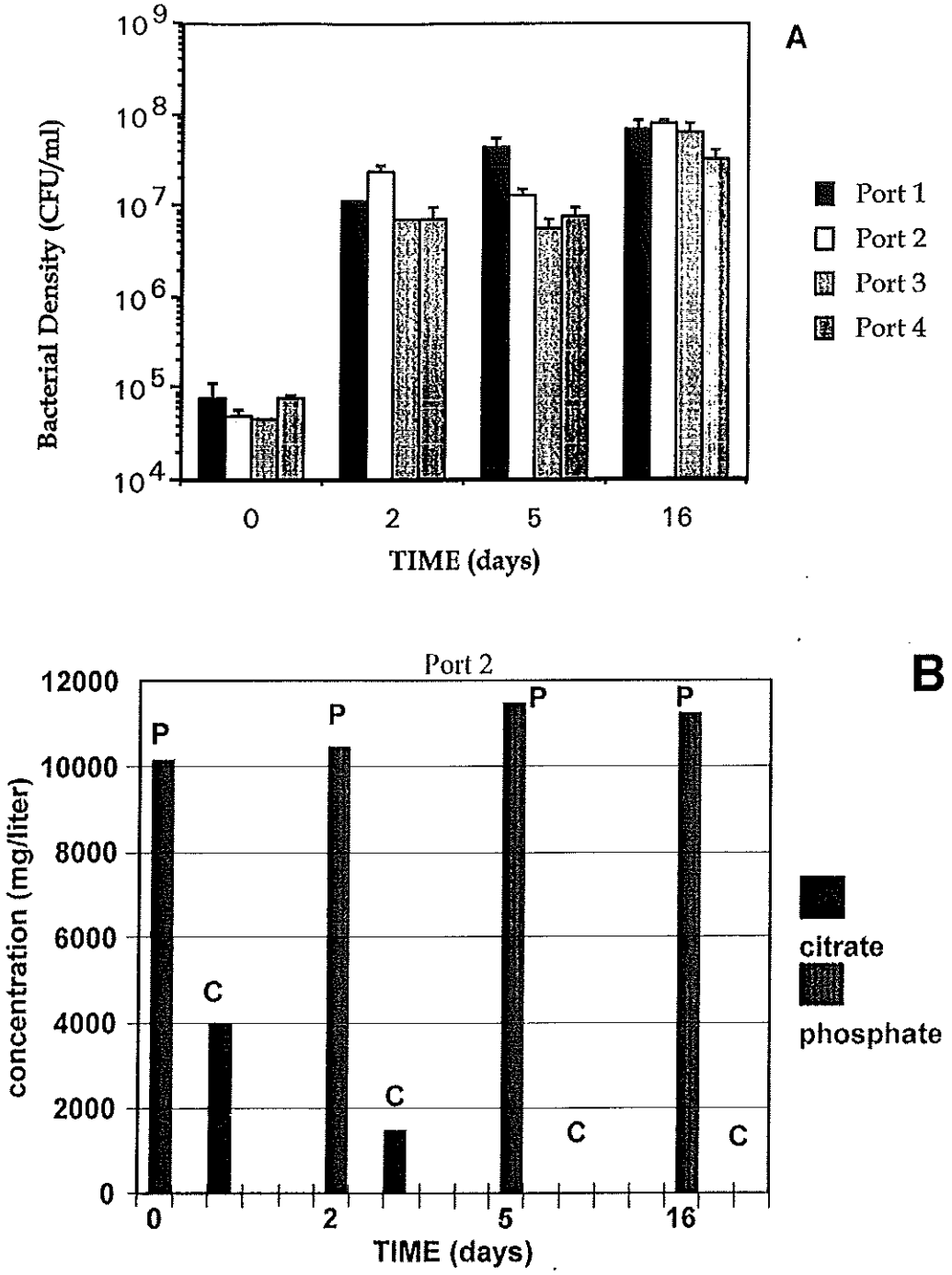

FIGURE 17.5
The column was inoculated with a starved cell suspension of *Klebsiella oxytoca* and incubated under no-flow conditions for 2 days, followed by 2 pore volumes of sodium citrate medium (SCM) and 2 more days of incubation at no flow. At day 5, continuous flow of SCM was initiated. Cells were recovered along the length of the column (ports 1, 2, 3, 4) after inoculation (time 0) and at 2, 5, and 16 days after inoculation (A). Typical citrate and phosphate concentrations were measured throughout a packed-sand column during nutrient resuscitation with SCM (B).

did not change appreciably over the 16-day-biobarrier-formation monitoring period, and provided evidence of homogeneous nutrient medium distribution (Figure 17.5B).

Bacteria were enumerated in sand samples taken from the columns after biobarrier formation (Figure 17.6). The distribution of bacteria was relatively uniform throughout the columns with a mean bacterial density of 108 CFU/g (wet-weight) of sand.

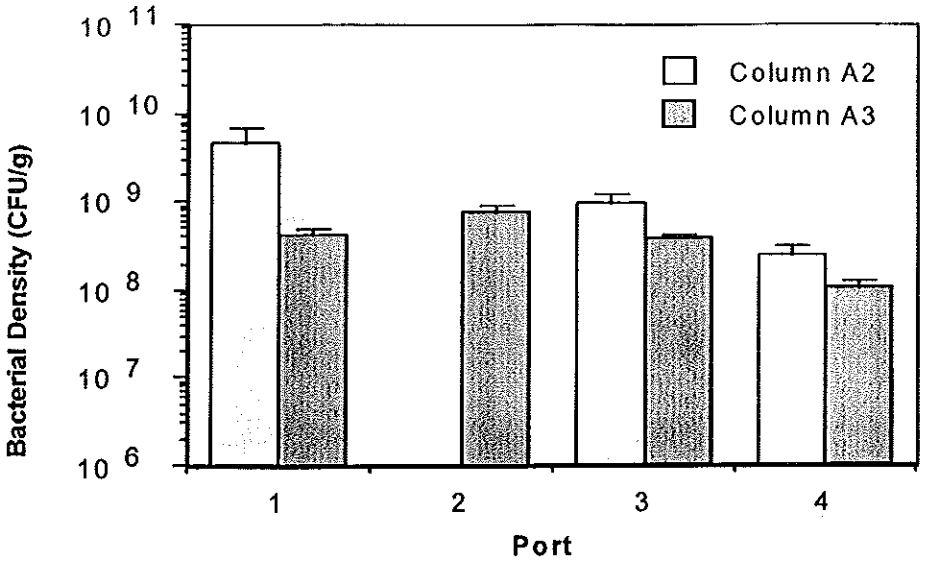

FIGURE 17.6
Bacterial densities in sand samples taken throughout columns A2 (control) and A3 (strontium challenge) after 96 days of biobarrier formation. Densities are reported as CFU per gram of wet sand. Note the even distribution of bacteria throughout the columns.

17.5.3 Reduction in Hydraulic Conductivity

Nutrient resuscitation of the starved bacterial inoculum resulted in a rapid reduction of hydraulic conductivity throughout the column length during the first 30 days. The hydraulic conductivity continued to decrease steadily at a much slower rate until reaching a relatively constant value after about 150 days. The net reduction in column hydraulic conductivity is approximately one order of magnitude (Figure 17.7). Stable hydraulic conductivity reductions were accompanied by a relatively constant number of culturable cells in the column effluent (107 CFU ml^{-1}).

Initial biobarrier development (0 to 50 days) indicates the column inlet sections reduce the hydraulic conductivity to a very low level. During continued barrier formation, the hydraulic conductivity at the effluent end of the column slowly decreases over an extended period (approximately 100 days) until a common hydraulic conductivity exists for the entire column. Biobarrier operation beyond 150 days indicates the column has a homogeneous biobarrier distribution and a common hydraulic conductivity throughout the column at approximately 0.1 cm/min.

Biobarrier persistence was evaluated by challenging the formed barrier with nutrient-free (DI-H_2O; challenge 1) and carbon-free (Mg/Fe solution; challenge 2) hydraulic flow (Figure 17.7). The hydraulic conductivity remained relatively constant for the first 5 days of challenge 1 and the first 10 days of challenge 2, and then rapidly increased in column sections farthest from the inlet. The effluent culturable cell density decreased from 10^7 to 10^6 CFU ml^{-1} during these starvation challenges. Following the barrier challenges, reintroduction of nutrient SCM medium resulted in a rapid reformation of the biobarrier throughout the column.

Resistance of the biobarrier to heavy metals was tested by addition of SCM containing 1 mg l^{-1} strontium (1 ppm) as strontium chloride, and SCM containing 1 mg l^{-1} cesium as cesium chloride (Figure 17.8). A carbon tetrachloride challenge was conducted by adding the solvent to the reservoir to provide a final target concentration of 200 mg l^{-1} carbon tetrachloride in SCM to the column. Neither of the two heavy metals nor the organic solvent had any measurable effect on biobarrier stability as measured by changes in hydraulic conductivity (data not shown).

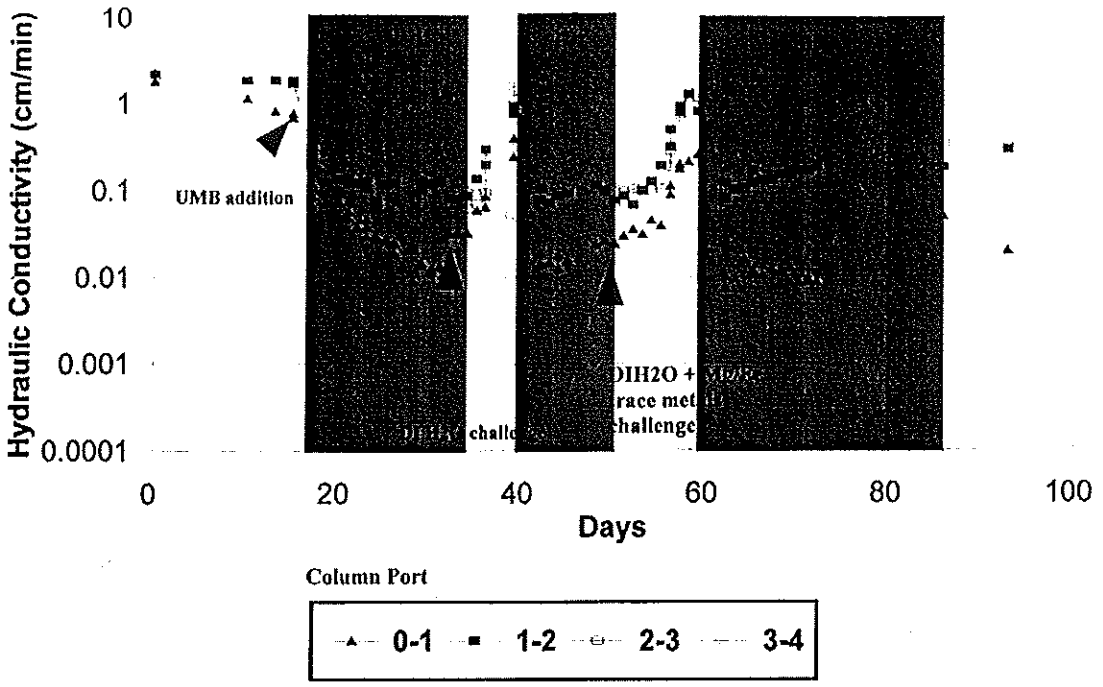

FIGURE 17.7
Biobarrier formation in a packed sand column from *Klebsiella oxytoca* fed sodium citrate medium (SCM). Nutrient-free (DI-water challenge) and carbon-free (Mg/Fe solution challenge) hydraulic flow resulted in a decrease in biobarrier performance. Biobarrier formation and performance returned quickly when SCM was provided (shaded regions).

17.5.4 Biobarrier Formation by Indigenous Microorganisms

An inoculated, nonsterile column packed with sand was fed SCM medium in a similar manner as the previously described column experiments. Another nonsterile column was flooded with the SCM medium, without inoculation, in order to observe the plugging pattern caused by indigenous organisms present in the water and in the sand itself. In the indigenous population column experiment, a reduction in hydraulic conductivity was achieved in the first section of the column compared to the remainder of the column (approximately two orders of magnitude greater; Figure 17.9). In the uninoculated column, the bacterial population was significantly higher near the column inlet and contained a relatively low number of streptomycin-resistant cells (Figure 17.10). In contrast, the bacterial population in the inoculated column was relatively uniform throughout the column length and contained a high proportion of streptomycin-resistant cells. We conclude that column flooding with UMB and nutrients results in a homogeneous plug while the simple resuscitation of indigenous bacteria lends to the formation of a shallow "skin" plug at the column influent.

17.6 Two-Dimensional Biobarrier Formation in Pilot-Scale Lysimeters

Two small pilot-scale lysimeters were designed and manufactured to facilitate evaluation of biobarrier performance in a two-dimensional configuration. This configuration

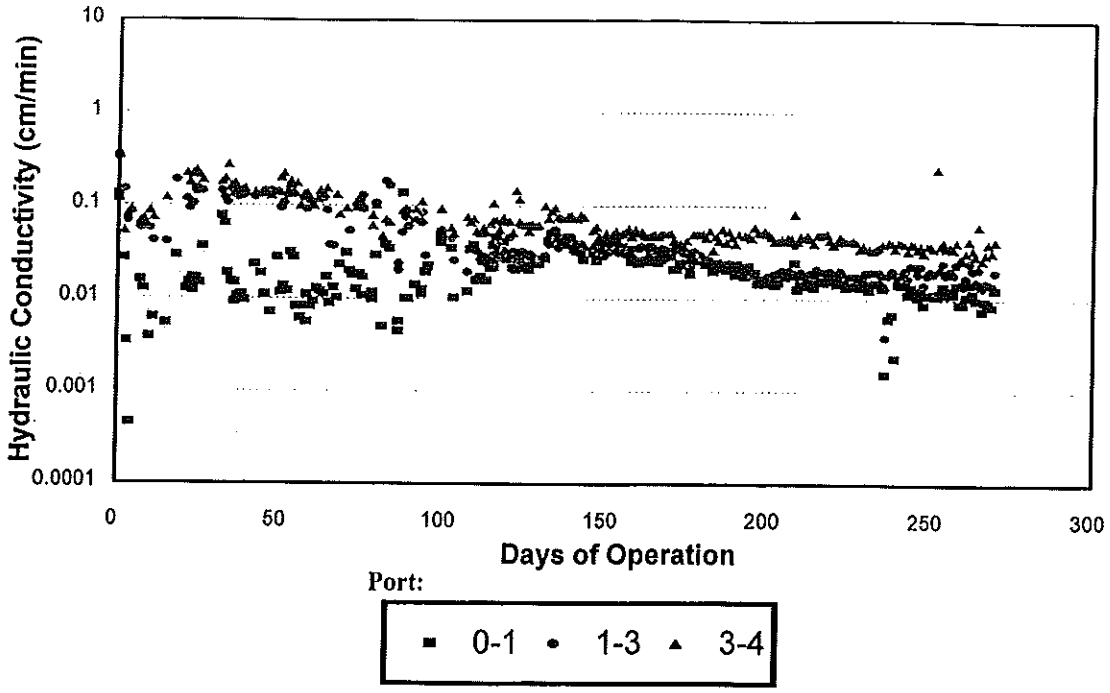

FIGURE 17.8
Established biobarrier resistance to 1 ppm cesium in sodium citrate medium. No deleterious effect of the heavy metal was noted during the 60 day challenge period (days 145 to 207).

provided hydraulic flow perpendicular to biobarrier formation, as compared to column design which consisted of hydraulic flow parallel and in conjunction with biobarrier formation. Evaluation of biobarrier performance in a two-dimensional configuration approximates field conditions more closely. As will be discussed later, the lysimeter provided a three-dimensional test of biobarrier performance. Two lysimeters were manufactured and used during these experiments to provide a side-by-side comparison of parameters affecting biobarrier formation and performance, such as heavy metal challenges and nutrient pulsing, and to provide destructive sampling opportunities (one reactor could be sampled while the other was maintained).

17.6.1 Lysimeter Design

The pilot-scale test lysimeters were manufactured from 0.95 cm and 0.48 cm 316 stainless steel (Figure 17.11). The inlet section was 91.4 cm wide by 61.0 cm deep by 15.2 cm long; the remainder of the reactor was 91.4 cm by 30.4 cm deep by 106.7 cm long, for an overall length of 122 cm. Four 7.6-cm flow distribution baffles are located on the top plate perpendicular to the flow direction at approximately 12.7, 41.9, 61.0, and 88.9 cm and 88.9 cm from the influent end of the top plate to limit sheet flow between the top of the sand and the top plate. A rigid support ran around the circumference of the reactor perpendicular to flow and approximately midway along the top plate, to provide support to the sides, base, and top plate. The support was approximately 1.3 cm high. The support also acted to disrupt flow along the walls, top, and base and redirect it into the sand fill.

Ten sampling ports were installed in two rows with logarithmically increased spacing from the inlet to the effluent end. Piezometer ports were installed in three evenly spaced rows across the reactor that had logarithmically increased spacing from inlet to effluent. Piezometer ports were also located on the hydraulic head tank and the effluent line, providing pressure-drop measurements between the head tank and

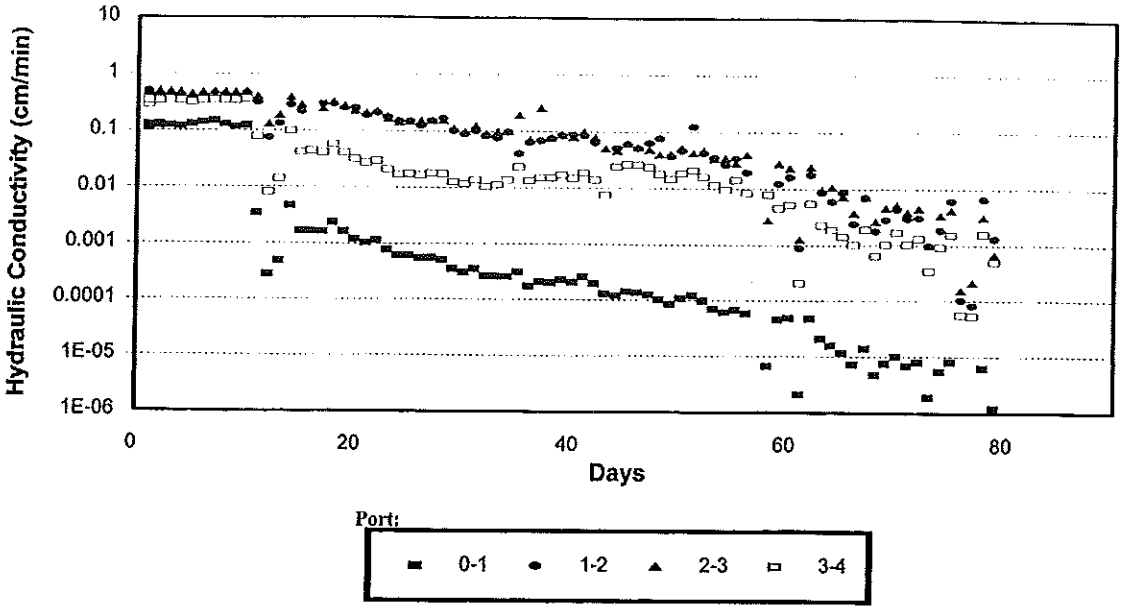

FIGURE 17.9
Skin-plug formation by indigenous bacteria in a packed sand column continuously fed with sodium citrate medium is indicated by the relatively high hydraulic conductivity drop between ports 0-1 and 1-2.

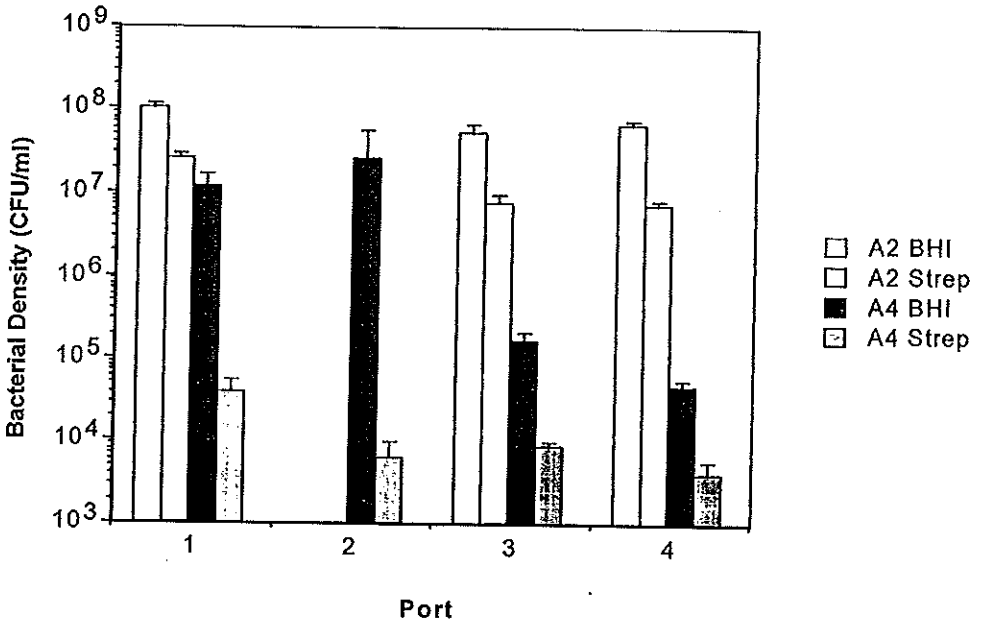

FIGURE 17.10
Total viable bacterial counts (BHI) and streptomycin-resistant bacterial counts (Strep) throughout biobarriers formed in a column (A2) inoculated with streptomycin-resistant *K. oxytoca* UMB and in a column (A4) that was not inoculated.

lysimeter effluent. Each reactor piezometer port was plumbed with a perforated 0.95-cm stainless steel tube to provide pressure-drop information across the full depth of the reactor.

A head tank (constant fluid level) provided reverse osmosis purified water at a constant head to the inlet of the reactor, simulating a constant-head hydraulic flow. This hydraulic gradient flow entered the reactor at the influent section of the reactor (approximately the first 15.2 cm of length), which was filled with coarse gravel to a depth of 45.7 cm. A total of 11 nutrient/inoculation injection ports were located in

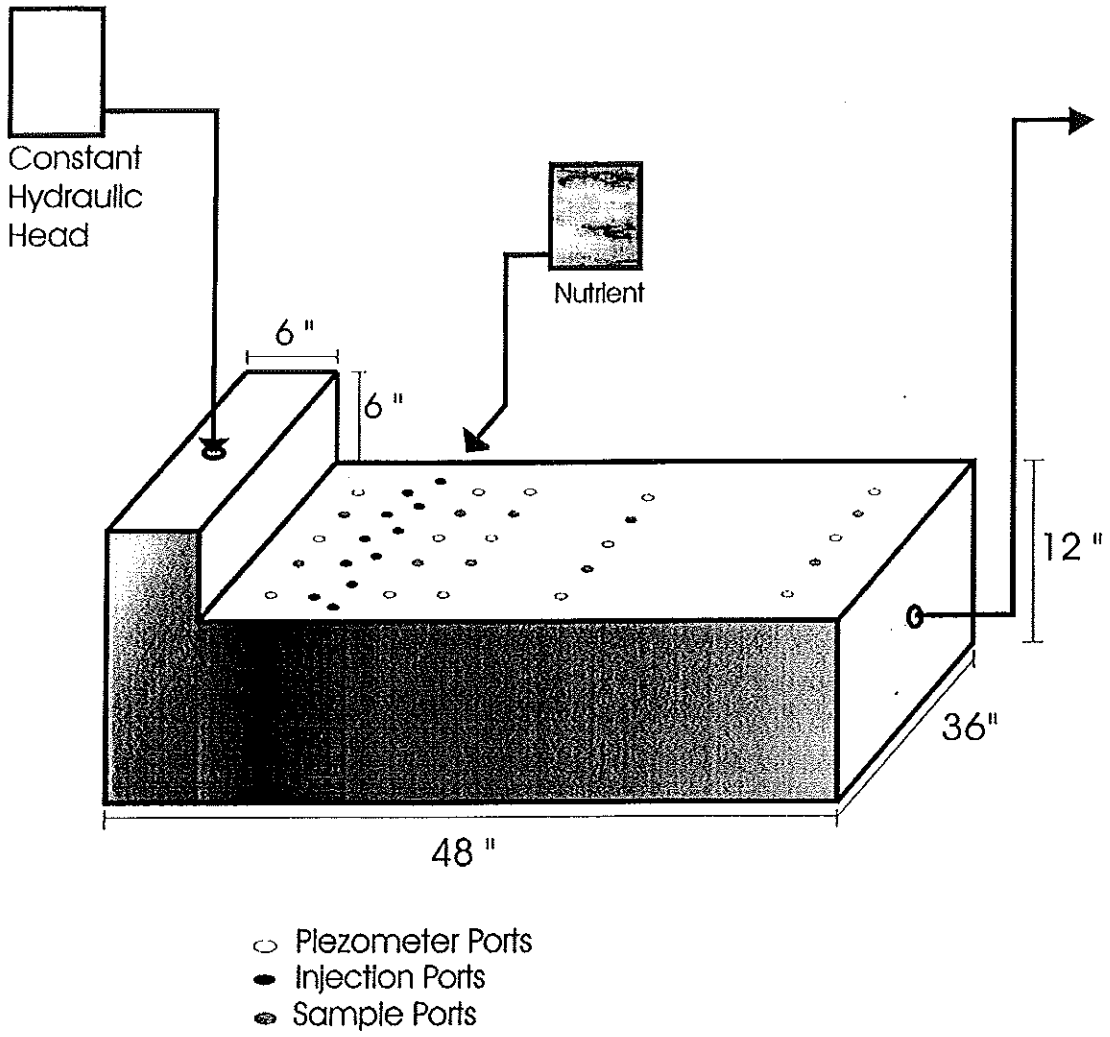

FIGURE 17.11
Pilot-scale lysimeter schematic. A constant-head hydraulic head tank provides reverse osmosis water as simulated groundwater flow. Nutrients and UMB are pumped into the injection ports downstream from the hydraulic head inlet. Biobarrier formation is monitored by flow rate measurements an piezometric monitoring of the hydraulic head throughout the lysimeter.

two rows (5 and 6 ports, respectively) near the inlet section of the reactor. These injection ports were also plumbed with perforated 0.95-cm stainless steel tube and are 2-way valved to a stainless T-fitting to provide sampling capabilities through a septum from the top and nutrient/inoculation injection into the "T".

Effluent from the reactor was collected on three levels by perforated 1.3-cm stainless steel tubing buried in coarse gravel in the last 15.2 cm of the reactor. The effluent head was maintained at a constant level approximately 3.8 cm below the head reservoir level.

The reactor was filled (except for the influent and effluent sections described above) with Ottawa Sand (F110) to its full depth. The hydraulic conductivity was calculated based on Darcy's Law (Equation 17.1) and the pore volume of the sand was determined through liquid displacement measurements. A pore volume of approximately 35% was measured for the F-110 sand used to fill the lysimeter beds. The initial overall hydraulic conductivity in the lysimeters was approximately 4.0 to 4.8 cm/min, respectively (calculation based on effluent flow rate and pressure drop across the entire reactor).

Tracer studies were conducted to evaluate the hydraulic flow characteriztics of the reactor prior to inoculation. A pulse of chloride as NaCl was introduced at varying

Hydraulic Head Tank Tracer Study

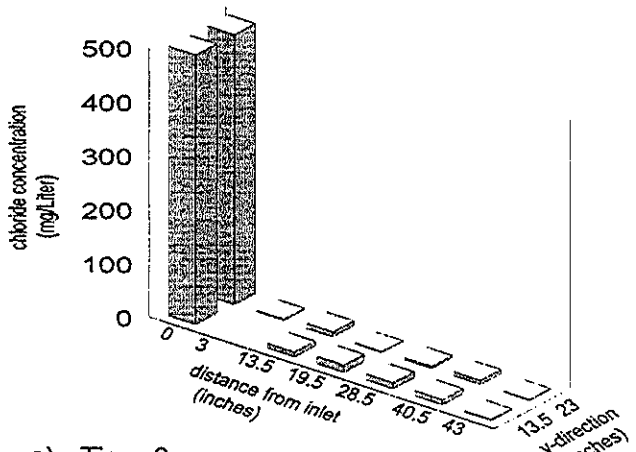

a) Time 0

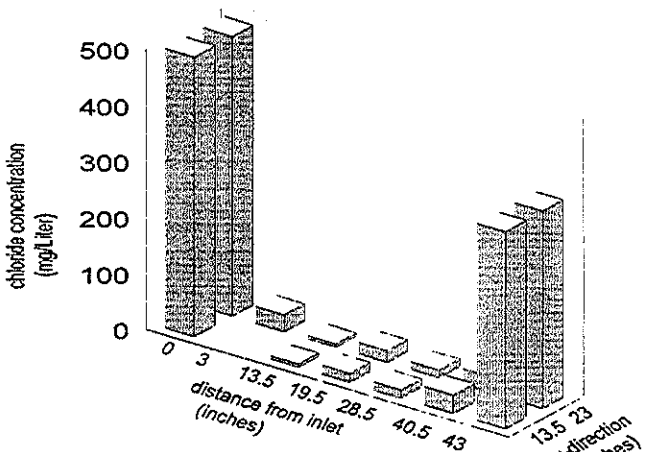

b) Time 330 minutes

Injection Tracer Study

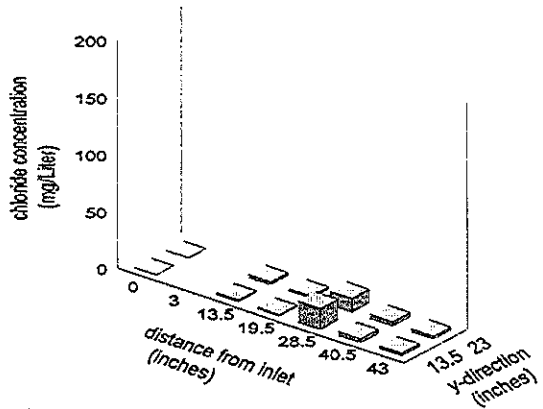

c) Time 0

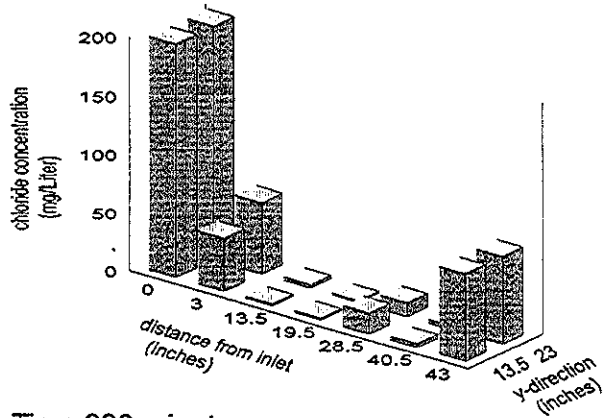

d) Time 330 minutes

concentrations into the hydraulic head tank and injection ports. The results of these tracer studies indicated preferential flow channels within the reactor beds (lysimeter II tracer results shown in Figure 17.12). These channels are indicated by zones of higher and lower salt concentration within the reactor, independent of their location. In addition, the effluent concentration increased to near-influent concentration much quicker than the sample ports along the length of the reactor. These results are indicative of heterogeneous flow in preferential flow channels compared to a uniform concentration gradient that would be expected under a homogeneous flow pattern.

Inoculation of the lysimeters was conducted by suspending the UMB culture in sodium citrate medium amended with a small amount of nitrate (mSCM) and pumping the suspension into the nutrient/inoculum injection ports using a multihead peristaltic pump. The injection flow rate was set to provide the inoculum flow rate at 10% of the total flow. The lysimeters were inoculated with a total of 0.2 pore volumes (PV) of UMB suspension [total of 2 PVs (inocula + hydraulic flow)] through the reactor. Following inoculum injection, mSCM injection commenced at the same flow rate. Nutrient injection continued until the reactor effluent flow rate equaled the injection flow rate, at which time nutrient injection was terminated. Nutrient injection at 10% of the pre-inoculation effluent flow rate was initiated as needed. The flow rate reduction achieved by the formation of a biobarrier in one lysimeter is plotted in Figure 17.13. The final flow reduction due to biobarrier formation was in excess of 99.99% of the initial flow. This flow reduction was maintained in excess of 99.9% for 4 months without further nutrient addition. The biobarrier challenge was conducted with 1 mg l^{-1} strontium (as strontium chloride) added to the hydraulic head tank. Column flow reduction continued during the strontium challenge (data not shown).

17.6.2 Column vs. Lysimeter Studies

Biobarrier persistence in the columns and lysimeters was significantly different. Column barriers appear to require continuous nutrient addition for barrier maintenance, while the lysimeter barriers were able to persist for a considerable period without nutrient addition. The persistence of the biobarriers in the lysimeters compared to the column experiments may be due to the higher head pressure continually present in the column reactor design. The difference is approximately 122 cm of head above the top of the 91.4-cm column compared to approximately 3.6 cm across the 122-cm length (91.4 cm of sand bed) of the lysimeters. The higher head provides a higher flow rate and pore velocity through the columns, which may increase the wash-out rate.

The results of the tracer studies and piezometric gradient data in the lysimeters indicate the presence of channels or wall flow. The presence of heterogeneous flow through the reactor cross section implies a three-dimensional reactor model rather than a two-dimensional model. The three-dimensional reactor model is therefore useful for field simulation of biobarrier formation and performance.

FIGURE 17.12
Lysimeter II chloride tracer study. Hydraulic head tank tracer study: 500 mg/l chloride as NaCl was added to the head reservoir. Sampling results are plotted for time 0 (a) and 1 pore volume (b). Injection port tractor study: 200 mg/l chloride was pumped into the injection ports at 10% of the combined flow rate (hydraulic + injection). The sampling results for time 0 (c) and 1 pore volume (d) are plotted. Reactor flow is characterized as primarily channel flow.

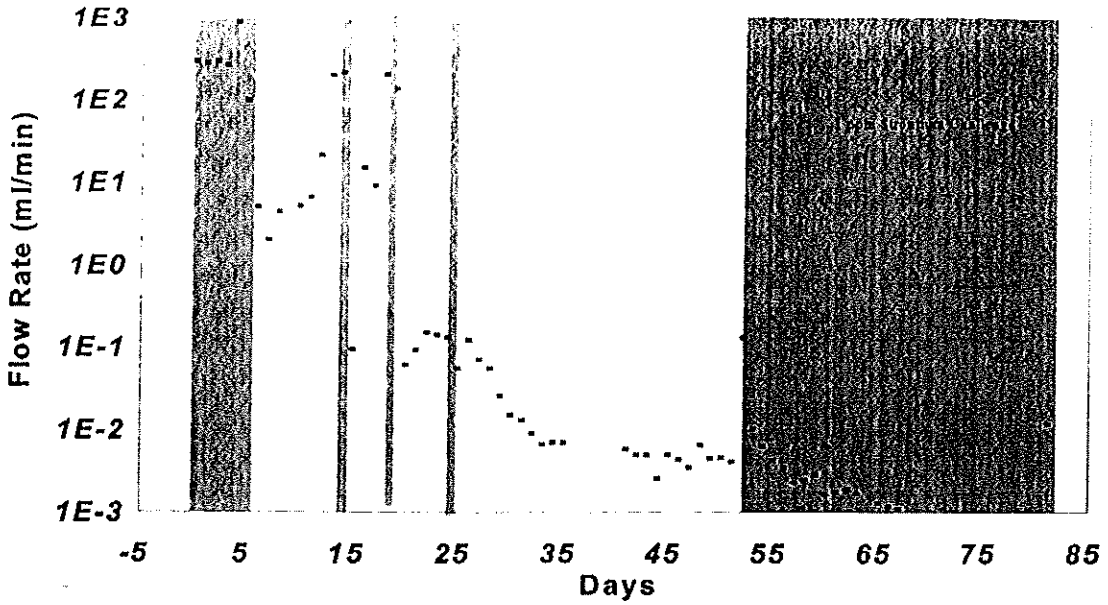

FIGURE 17.13
Lysimeter II effluent flow rate vs. time. UMB/nutrient addition occurred at time 0. Continuous nutrient pumping through the injection ports at 10% of the combined flow rate (hydraulic + injection) during the first 7 days and pulse injection at 3 time periods thereafter (shaded regions) reduced the flow rate 99.999%. A strontium challenge at 1 mg/l in the hydraulic flow was initiated on day 52 (cross-hatch region) and this toxic metal did not affect the biobarriers.

17.7 Conclusions

17.7.1 Biobarrier Development

Initial biobarrier development is a rapid and effective method for reducing the hydraulic conductivity throughout the length of the 3-ft packed sand columns and small lysimeters. An initial reduction in the hydraulic conductivity to less than 10% of the original value was observed in all columns and reactors, and reduction to less than 0.0001% of the initial hydraulic conductivity was obtained in the lysimeter studies.

17.7.2 Biobarrier Maintenance

Reduced reactor flow rates during biobarrier persistence leads to low nutrient addition flow rates and, therefore, minimal nutrient requirements for maintenance (less than 10% of the original liquid flow through the column). However, starvation conditions had a deleterious effect on biobarrier effectiveness in one-dimensional column models, suggesting that nutrient supply is required for biobarrier maintenance under high hydraulic head situations. The results of the column and lysimeter experiments suggest wash-out of the barrier is a function of the hydraulic head and flow rate through the formed barrier. After formation, biobarrier persistence under low flow conditions may require only limited nutrient addition to maintain extremely low hydraulic conductivities. In addition, extended operation of an engineered biobarrier resulted in a homogeneous biobarrier distribution throughout the 91.4-cm packed sand columns and 122-cm lysimeters.

17.7.3 Biobarrier Heavy Metal and Organic Solvent Challenge

Biobarrier performance and formation was not altered by the presence of heavy metal contaminants (strontium and cesium) at 1 ppm levels for periods up to 120 days, or influenced by the presence of carbon tetrachloride at concentrations of 100 mg/l for extended periods and up to 300 mg/l for short periods.

17.7.4 Three-Dimensional Flow Simulation

Documentation of the presence of flow heterogeneities in the pilot-scale lysimeters indicates that a three-dimensional flow pattern was developed, and was effectively plugged, using the biobarrier technology. Preferential wall or flow channeling was significantly reduced in addition to low flow zones within the sand.

Overall, these results indicate the hydrodynamic properties of porous media can be manipulated using microbial biobarriers, and these barriers may be an effective technology for the containment of groundwater contaminants. The UMB-based biobarrier technology is being considered for commercial use in the selective plugging of high-permeability water breakthrough zones in secondary oil recovery by water flooding. A very similar use of the technology is being considered for the construction of barriers to protect natural ecosystems (e.g., rivers and lakes) from pollutant plumes in approaching groundwater. Plugging biobarriers are being considered as reinforcements to the linings of landfills, especially those containing toxic organic molecules and/or heavy metals. UMB introduction, with subsequent nutrient infusion, has been suggested as a means of plugging water "fingering" channels in earthen dams and berms (Lappin-Scott and Costerton, 1992). UMB have been suggested as a delivery mechanism for the introduction of pollutant degrading/reducing organisms into subsurface plumes of organic and metallic pollutants. Perhaps the most intriguing possibility is using UMB to reduce indigenous metals (e.g., iron) in the path of groundwater containing chlorinated organic molecules and/or oxidized heavy metals. These reduced indigenous metals (e.g., ferrous iron) would then reductively dechlorinate the organic pollutant (Caccavo et al., 1996; Gorby et al., 1995) and/or reduce the mobile heavy metals to produce immobile crystals of insoluble metal salts. A mixture of UMB and vegetative bacterial cells could readily be used to produce a zone of nutrient-stimulated metabolic activity at the surfaces of mine tailings that would serve as an oxygen-consuming "cap" that would prevent the penetration of oxygen and the consequent development of acid mine drainage (Blenkinsopp et al., 1991).

Acknowledgments

This research was funded by DOE through MSE, Inc. under agreement 95-C213-CR, and by the U.S Environmental Protection Agency under assistance agreement R-815709 to Montana State University through the Hazardous Substance Research Center for U.S. EPA Regions 7 and 8, headquartered at Kansas State University.

The authors wish to acknowledge the contributions of personnel at MSE, Inc. and at the Center for Biofilm Engineering (an NSF-supported Engineering Research Center under Cooperative Agreement EEC-8907039) located at Montana State University.

References

Blenkinsopp, S.A., D.C. Herman, and J.W. Costerton, The Use of Biofilm Bacteria to Exclude Oxygen from Acidogenic Mine Tailings, in Proc. *Second Int. Conf. Abatement of Acidic Drainage*, Montreal, pp. 369-377, 1991.

Caccavo, F., Jr., N.B. Ramsing, and J.W. Costerton, Starvation and Resuscitation of the Dissimilatory Metal-Reducing Bacterium Shewanella Alga Strain BrY., Manuscript Submitted.

Cunningham, A.B., E.J. Bouwer, and W.G. Characklis. Biofilms in porous media, in *Biofilms*, W.G. Characklis and K.C. Marshall, Eds., John Wiley & Sons, New York, 1990, pp. 697-732.

Cunningham, A.B., W.G. Characklis, F. Abedeen, and D. Crawford. Influence of biofilm accumulation on porous media hydrodynamics, *Environ. Sci. Technol.*, 25:1305-1310, 1991.

Cusack, F., S. Surindar, C. McCarthy, J. Grieco, M. DeRocco, D. Nguyen, H. Lappin-Scott, and J. W. Costerton, Enhanced oil recovery — three-dimensional sandpack simulation of ultramicrobacteria resuscitation in reservoir formation, *J. Gen. Microbiol.*, 138:647-655, 1992.

Gorby, Y.A., D. J. Workman, S.E. Amonette, and J.S. Fruchter, Transformation of carbon tetrachloride by biogenic Fe(II), in *Emerging Technologies in Hazardous Waste Management, VII*, Division of Industrial & Engineering Chemistry, American Chemical Society, Washington, D.C., 1995, p. 593.

Kjelleberg, S., *Starvation in Bacteria*, Plenum Press, New York, 1993.

Lappin-Scott, H.M., F. Cusack, and J.W. Costerton, Nutrient resuscitation and growth of starved cells in sandstone cores: a novel approach to enhanced oil recovery, Appl. *Environ. Microbiol.*, 54(6):1373-1382, 1988.

Lappin-Scott, H.M. and J.W. Costerton, Ultramicrobacteria and Their Biotechnological Applications, *Curr Opinion Biotechnol.*, 3:283-285, 1992.

MacLeod, F.A., H.M. Lappin-Scott, and J.W. Costerton, Plugging of a rock model system by using starved bacteria. Appl. *Environ. Microbiol.*, 54(6):1365-1372, 1988.

McKinley, V.L., J.W. Costerton and D.C. White, Microbial biomass, activity, and community structure of water and particulates retrieved by backflow from a waterflood injection well, *Appl. Environ. Microbiol.*, 54(6):1383-1393, 1988.

Novitsky, J.A. and R.Y. Morita, Morphological characterization of small cells resulting from nutrient starvation of a psychrophilic marine vibrio, *Appl. Environ. Microbiol.*, 32:617-622, 1976.

Reichert, P., AQUASIM — a tool for simulation and data analysis of aquatic systems, *Water Sci. Technol.*, 30(2):21-30, 1994.

Rittmann, B. E., The significance of biofilms in porous media, *Water Resour. Res.*, 29(7):2195-2202, 1993.

Shaw, J.C., B. Bramhill, N.C. Wardlaw, and J.W. Costerton, Bacterial fouling in a model core system, Appl. *Environ. Microbiol.*, 49(3):693-701, 1985.

Stoodley, P., D. DeBeer, and Z. Lewandowski, Liquid flow in biofilm systems, Appl. *Environ. Microbiol.*, 60(8):2711-2716, 1994.

Wanner, O., A.B. Cunningham, and R. Lundman, Modeling biofilm accumulation and mass transport in a porous medium under high substrate loading, Biote*chnology and Bioengineering*, 47:703-712, 1995.